Energy Reports 9 (2023) 5111–5124

Contents lists available at ScienceDirect

Energy Reports

journal homepage: www.elsevier.com/locate/egyr

Research paper

Performance comparison of pelamis, wavestar, langley, oscillating water column and Aqua Buoy wave energy converters supplying islands energy demands

Mohammad Hossein Jahangir *, Reza Alimohamadi, Mohammad Montazeri

Renewable Energies and Environmental Department, Faculty of New Sciences and Technologies, University of Tehran, Tehran, Iran

ARTICLE INFO

Article history:
Received 24 September 2022
Received in revised form 15 November 2022
Accepted 6 April 2023
Available online xxxx

Keywords:
Hybrid renewable energy system
Wave energy converters
Techno-economic analysis
Cost of energy

ABSTRACT

Considering the potential of renewable resources in the Persian Gulf islands, this study proposed a hybrid system in two scenarios of limited and unlimited generators. Also, the five wave energy converters' technical and economic impact was evaluated as a new approach to sustainable electricity generation. In addition, a comprehensive sensitivity analysis was provided for the net present cost relative to cost changes of wave converters. Results indicated that in the scenario of limited generator, the hybrid system, including the photovoltaic panel, the diesel generator, and the Wavestar wave energy converter with a cost of energy 0.224 $/kWh and net present cost of 11 M$ and the unlimited scenario, the photovoltaic panel, the diesel generator, and AquaBuOY wave energy converter hybrid system with the cost of energy 0.209 $/kWh and net present cost 10.3 M$ are the most optimal scenarios. Also, the OWC-SPA converter had the largest electricity generation among the five selected converters. In addition, in the optimal scenario, the cost of energy of the Wavestar wave converter was 0.385 $/kWh, and in the second scenario, the cost of energy of the AquaBuOY wave converter was 2.05 $/kWh. The cost of energy for the photovoltaic panel was 0.0244 $/kWh and it was 0.0394 $/kWh for diesel generator. Finally, the range of changes in the net present cost was estimated from 10.3 M$ to 13.9 M$, despite the fluctuations in wave converter costs.

1. Introduction

Nowadays, there is a significant tendency to use renewable energies (Fakouriyan et al., 2019); because they can lead to substantial macroeconomic benefits by affecting Gross Domestic Product (GDP), unemployment, and trade balance (Andini et al., 2019). Also, they can provide energy security in terms of environment and sustainability (Middleton, 2018). In addition to the high cost of renewable energy (Krozer, 2013), their intermittent nature is one of the main factors in the continuous production of energy from these sources. Overcoming the risks associated with fluctuations in energy production from renewable sources is provided by integrating different renewable sources into a single set called a hybrid energy system. Two or more energy sources connect through substations, generate electricity, and transmit it to the grid (Carvalho et al., 2019).

According to the reports of REN21 (Renewable Energy Policy Network for the 21st Century), in 2008, approximately 6% of the total energy consumed came from modern renewable energy (hydropower, ocean energy, biomass, wind, solar, geothermal, etc.) (Ren21, 2010). In 2017, this percentage reached 10.6 (Ren21, 2019). Also according to the latest published energy balance sheet (National Energy Balance of Iran for 2016), between March 20, 2016, to 2017, Iran's electricity generation from renewable power plants saw a growth of 16.2% compared to the previous year, which indicates an increasing trend in energy use (Energy National Balance Sheet of Iran for 2016, 2016). Also, Oceans have several inherent forms of energy: hydrodynamics (waves and tides), heat (temperature gradients between different water depths), and waves (Ocean Wave Energy, 2016; Renewable Energy Sources, 0000). The energy in oceans is estimated to be far greater than the world's predictable demand for electricity. However, not much attention has been paid to the wave's energy. The current use of marine energy has a small share of the global energy supply. About 0.5 GW of commercial offshore power generation is currently installed, and another 1.7 GW is under construction (Wilberforce et al., 2019).

Wave power, meanwhile, is an emerging technology, and several studies have been conducted on the integration of wave

* Corresponding author.
E-mail address: mh.jahangir@ut.ac.ir (M.H. Jahangir).

https://doi.org/10.1016/j.egyr.2023.04.051

Nomenclature

A	Area (m^2)
C_{Bat}	Battery capacity (kJ)
f	Annual Inflation rate (%)
f_{PV}	PV derating ratio (%)
G	Sun Radiation (kW/m^2)
H	Height (m)
i°	Nominal interest rates (%)
IT	Indirect radiation (W/m^2)
n	Project lifetime (year)
P	Power (kW)
R_{Comp}	Component lifetime (year)
T	Temperature (°C) and periodicity (s)
V	Speed (m/s)
J	Medium energy flux (W)
Y_{PV}	Rated capacity of PV (%)
C_g	Group speed (m/s)
P	Pressure (pa)
w	Capture width (m)
S_B	Control Surface
ρ	Density (kg/m^3)
L_{max}	Absorption width at maximum Power (m)
E	Energy (J)
B	Characteristic dimension (m)

Greek symbols

β	Photovoltaic panel absorption (%)
α	Temperature coefficient (%/°C)
ω	Frequency (rad/s)
Ø	Wave potential
λ	Wavelength (m)
η	Efficiency (%)

Abbreviations

WT	Wind Turbine
COE	Cost of Energy ($/kWh)
DFC	Diesel fuel consumption (l/h)
DG	Diesel generator
WEC	Wave energy converter
IC	Initial cost
LCOE	Levelized cost of energy
NOST	Nominal operation cell Temperature (°C)
NPC	Net present cost ($)
OS	Oscillating wave
PV	Photovoltaic panel
Bat	Battery
DFC	Diesel fuel Consumption
IC	Initial capital
RF	Renewable fraction
FSVP	Floating solar PV

energy, photovoltaic, and wind power. The wind is created by the difference in temperature on the surface of the oceans and seas and causes the formation of the ocean and sea waves. These waves carry both kinetic energy and potential energy (Zhang et al., 2018). Technology developers and researchers propose several methods that use wave energy converters (WEC) to convert wave energy into electricity. These systems can be classified as oscillating water columns, attenuators, point absorbers, overtopping, etc. (Blue to Green, 2011; Sang et al., 2017). Many of these devices have been installed and tested on real scales, laboratories, or specific test sites (Laws and Epps, 2016).

Talaat et al. have proposed dynamic and control Scenarios of a combined wind, solar, and wave energy system to find the effectiveness of the simulated converter. In addition, an experimental test platform has been developed for these three renewable energy sources to study how to integrate and standardize their energy production and evaluate the simulation Scenario. The results indicated that the simulation Scenario is practical, and this Scenario can be used to combine the three proposed energy types (Talaat et al., 2019). Bozzi et al. have examined the potential of the Mediterranean Sea to generate electricity from the wave. For this purpose, the performance of a set of offshore wave energy converters (WECs) along the Mediterranean coastline was evaluated based on 37-year-old prefabricated wave data and general WEC performance data. The results indicated that a large part of the Mediterranean coastline could be successfully exploited with proper versions of WECs. In particular, the six wave power technologies studied can reach a capacity factor of more than 0.2 along 40% of the shoreline, and the three wave converters AquaBuOY, Pelamis, and Wavebob can use a capacity factor of more than 0.3 in 80% of the studied locations (Bozzi et al., 2018).

Researchers in the United States Department of Statistics analyzed the integration of wave energy into the grid, along with wind and solar energy (Reikard et al., 2015); Insur Haryuda reviewed the designing, optimization, and controlling of a combined wave, wind, and solar system to meet the energy demand of coastal areas. The results indicated that the combined system, including solar, wave, and battery with inverter system, is economical and environmentally, provides more energy, and Causes less environmental pollution (Haryuda et al., 2019).

Land analyzed the integration of large-scale wind, solar, and wave energy into a Danish reference system. The results indicated that the optimal System would occur when wind power generates 50% of total electricity from renewable energy sources. In addition, the Hybridization wave and solar depend on the total amount of electricity generated from renewable sources. When the total input of renewable energy sources is less than 20%, PV and wave power should provide 40% and 10% of energy, respectively. PV should provide 20% and wave power 30% of energy when the total input is more than 8% of demand (Lund, 2006).

Rodriguez Delgado investigated the effect of wave height on the eleven vibrates used in Playa Granada according to the spectral propagation Scenario. They pursued two main goals: calculating electricity generation and protecting the coastal zone. The results emphasized that the farm would lead to the protection of coastal structures (Rodriguez-Delgado … and of C., 2019).

In Iran, due to the accessibility of the Caspian Sea, with average wave power between 1.5 to 3.5 kWh in neighboring cities (Jahangir and Mazinani, 2020), the Persian Gulf, with average wave power between 0.3 to 3 kW/m (Kamranzad and Chegini, 2014), and the Gulf of Oman With an average wave power of more than 2 kW/m (Rashid et al., 2011), Hybridize wave energy with other renewable sources can be considered a good way to increase the benefits of hybrid systems in these coastal areas. M. Jahangir et al. considered an HPWEC system and extracted the corresponding hydrodynamic equations, after which, taking into account the obtained equations and raw data, all possible Scenarios for the hypothetical system were determined. Then, considering the Top-Down clustering method, the optimal state of the system and its related parameters were identified. The

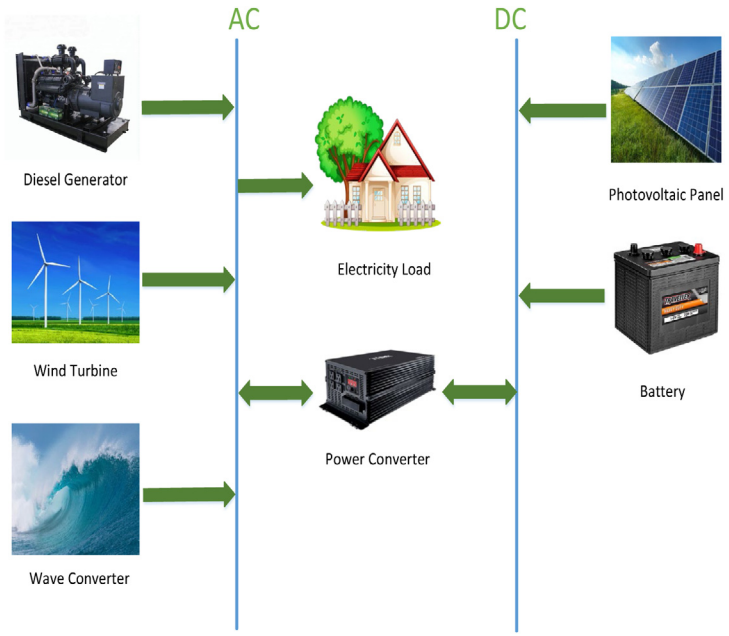

Fig. 1. System simulation in Homer software.

result was that the Top-Down clustering method is effective as one of the data mining approaches and can analyze all linear and nonlinear systems (Jahangir and Khatibi, 2020).

M. Jahangir et al. performed a technical, economic, and environmental analysis of a hybrid system, including a wind turbine, a photovoltaic panel, a Pelamis wave energy converter, and a battery to provide power to people living in coastal areas. The results showed that the best option, economically, to supply electricity with an independent combined system is a combination of wind, solar, and battery systems (Jahangir et al., 2020b).

M. Jahangir et al. examined a combination of renewable sources with higher reliability, cleaner, and more efficiency. In that study, two coastal areas with different climatic conditions were selected and analyzed technically, economically, and environmentally according to both in-network and off-network conditions. The renewable hybrid system included solar panels, wind turbines, wave converters and large-scale batteries. In order to improve the performance of the combined system in off-grid Scenario, the diesel generator was used in two scenarios as primary and backup equipment. Then, to generalize other results in other parts of the world, a comprehensive sensitivity analysis was performed on the impact of economic and technical parameters of the system (Jahangir et al., 2020a).

As seen from previous studies, there are fundamental challenges to hybrid converter-based hybrid systems that have not been addressed. According to this issue, simultaneous technical-economic analysis of selected marine wave energy converters based on data from the Iranian Institute of Atmospheric Science and Oceanography to provide part of the electricity required for Lavan Island has been investigated. The purpose of this research is to participate in logical and evidence-based arguments that support the development and forthcoming decisions on the "hidden" opportunities of the emerging wave energy industry to find a suitable hybrid system, including wave converters compatible with regional sea characteristics. Combined with other renewable sources to lead to sustainable and environmentally friendly energy production for the 2500 inhabitants of Lavan Island. In order to maintain the network, the effect of the diesel generator as the main and supporting component in the said hybrid system is also investigated. Finally, sensitivity analysis on the cost of wave converters is also performed.

The use of renewable energy to generate power, in addition to preventing the uncontrolled emission of greenhouse gases, can also help the energy independence of remote areas, not be affected by fluctuations in fossil fuel prices, and also help to employ skilled labor in those areas. Slowly, Therefore, trying to make maximum use of various renewable sources (especially wave energy in island areas such as Lavan) is very important.

2. Methods

2.1. System descriptions and scenarioling

This research has been done to design and Scenario a renewable hybrid system including solar photovoltaic panels, wind turbine, wave converter, and generator to provide electricity demand for 2500 people of Lavan Island located in the Persian Gulf (Jahangir et al., 2020b). Fig. 1 shows the proposed Scenario of energy systems. In this system, diesel fuel is used as an available source to supply part of the load. The battery system is used to meet uniform demand and increase network reliability. It should be noted that the equipment of the combined power system has been selected based on the energy sources available in the study area. A number of developed devices were chosen for the WEC system and then used in simulations based on the area wave potential. In this regard, the purpose of this study is to investigate the final cost of energy for the hybrid power supply system in Lavan Island in two constraints for the generator and non-constraint and to evaluate the ability of WEC hybridization with other conventional renewable systems.

2.2. Case study

Lavan is one of the most critical and strategic islands in the Persian Gulf in terms of oil resources, and it has caused most of its parts to be occupied by the Ministry of Oil and has caused a lot of environmental pollution for it (Lavan, 0000). Lavan Island is located at 53.28 degrees east longitude and 26.8 degrees north latitude. The area of this island is 81 km^2, which makes it the third largest island in the Persian Gulf Fig. 2. The island has a population of about 2500 (Google Search, 0000). However, many

Fig. 2. Aerial map of Lavan Island (google map - Google Search, 0000).

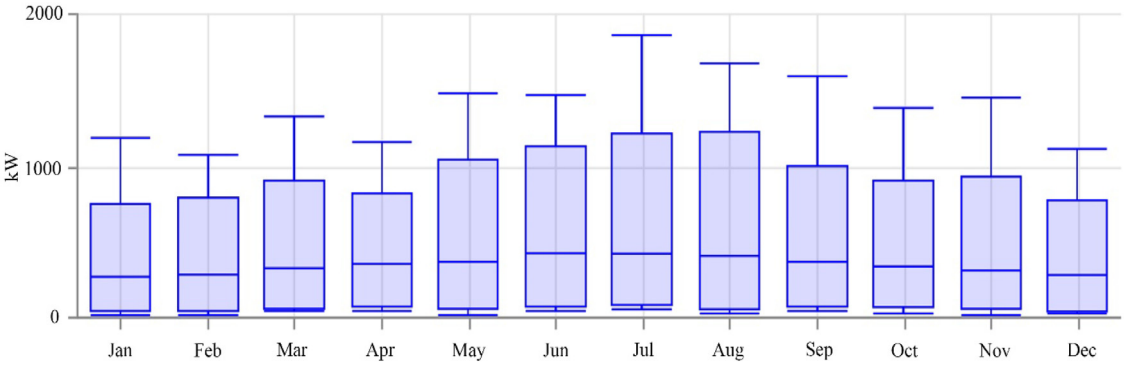

Fig. 3. Monthly electricity consumption profile of Lavan Island (HOMER, 0000).

engineers and technicians visit the island annually due to the abundance of oil and gas resources. Therefore, paying attention to meeting the needs of this population (residential) is on the agenda.

2.3. Electrical load

Although most areas of Iran benefit from electricity within the network, a large number of villages are deprived of electricity because they are located in remote areas, or their network reliability is low. Due to the hot and dry climate in Iran, electricity consumption obviously reaches its peak in the hot months. In most remote coastal areas, electricity consumption for cooling has increased during the warmer months. In recent years, power transmission lines have been provided to most parts of Iran. However, because most power plants are located in the country's central regions, cities with smaller populations have little priority for power transmission lines. Based on the impact of various local resources on the system's cost-effectiveness and on the consumption specifications for Lavan Island in accordance with Fig. 3, the electricity consumption specifications for Lavan Island have been designed. This time it is scaled for 700 households with an average electricity consumption of 12.5 kWh per day (Jahangir et al., 2020b). The load characteristics show an average consumption of 8750 kWh per day.

2.4. Renewable resources in Lavan Island

Climate information is very effective in Scenarioling the energy system, including solar radiation, temperature, wind speed, period, and wave height. In Lavan Island, according to NASA average annual solar radiation is 6.10 (kWh/m^2/day), wind speed is 5.38 (m/s), and temperature is 27.34 °C (Nasa, 2019). The average annual height and period of waves that have been extracted from the sources of the Iranian Institute of Atmospheric Sciences and Oceanography (INCOD, 0000) are 1.125 (m), 5.18 (s), which indicates that Lavan Island has good renewable resources Table 1. It shows the monthly average information of each resource.

2.5. Wave energy converter selection

The wave energy converter converts the waves' mechanical energy into electrical energy (Jahangir et al., 2020a). Several wave converters have been selected with the available information to find the right wave device to combine with other renewable sources. Then, according to the potential waves in Lavan Island, the power curve of five wave converters is chosen, and its efficiency in combination with other renewable sources is investigated. Five wave converters of Pelamis, Wavestar, Langlee, SPA-OWC and AquaBuOY are briefly introduced in the following. Among the five selected wave converters, Pelamis and Wavestar converters are of attenuator type, Langlee converter is of oscillating wave surge converter type, SPA-OWC converter is of water oscillating column type and AquaBuOY converter is of point absorber type Fig. 4.

Eq. (1) shows the maximum theoretical power extractable from sea waves:

$$P_{\max} = \frac{\rho g^2 T H^2}{64\pi} . L_{\max} \tag{1}$$

where P_{max}(w) is the maximum power that can be extracted, ρ is the Water density, g (m/s^2) is the gravitational acceleration, T

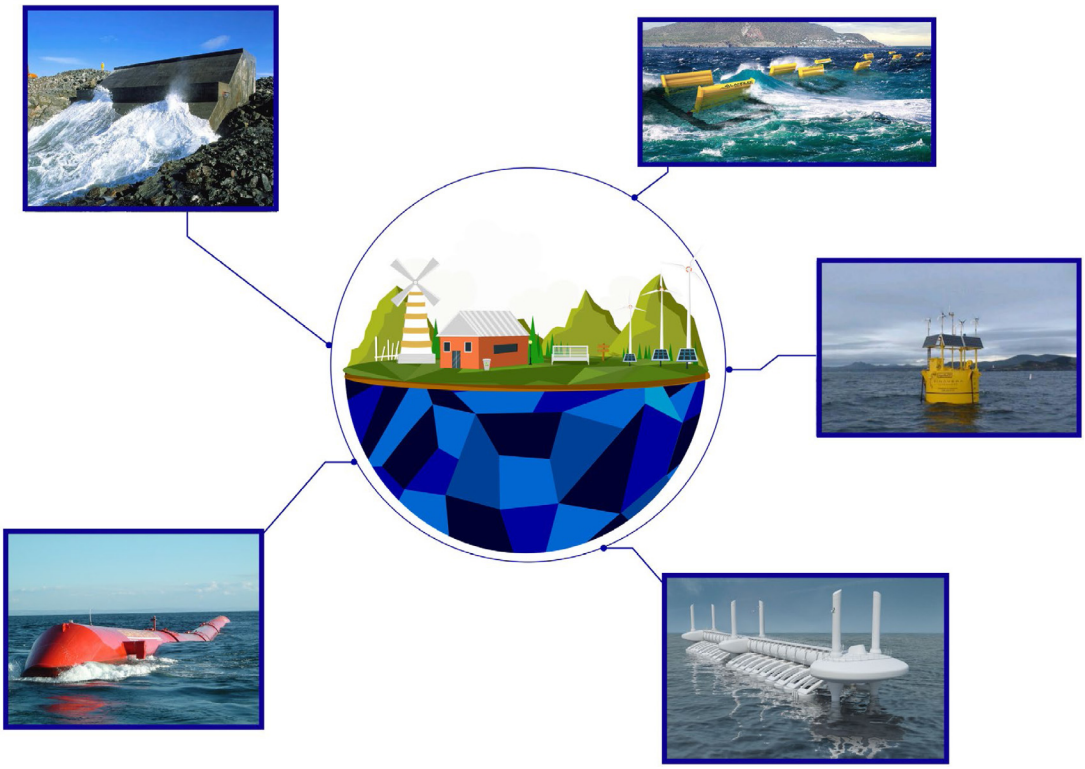

Fig. 4. Feasibility study of 5 wave converters for Lavan Island.

Table 1
Average monthly renewable resources and climatic conditions of the Lavan Island.

Month	Daily radiation (kwh/m^2/day)	Clearness index	Daily temperature (°C)	Wind speed (m/s)	Wave period (s)	Wave height (m)
January	4.050	0.630	18.690	5.240	5	1.4
February	4.960	0.653	19.450	5.970	5	1.3
March	5.780	0.637	22.080	5.670	6	1.2
April	7.000	0.676	26.630	5.490	5.3	1.250
May	7.660	0.692	31.470	6.040	4.9	1.6
June	7.990	0.707	33.440	5.910	5	1.1
July	7.750	0.695	34.350	5.520	5	0.650
August	7.120	0.673	34.190	5.380	5	0.650
September	6.690	0.706	32.420	4.960	4.9	1.150
October	5.810	0.725	29.270	4.620	4.9	0.9
November	4.600	0.689	25.170	4.530	6	1.3
December	3.770	0.622	20.930	5.170	5.2	1

Table 2
Hydrodynamic efficiency suitable for different types of WEC systems.

The most suitable efficiency equation	Converter operation type
$\eta_1 = 1.4B + 2.1$	Oscillating water column (SPA-OWC)
$\eta_1 = 1.3B + 5.6$	Attenuator (Pelamis, Wavestar)
$\eta_1 = 1.4B + 2.1$	Point absorber (AquaBuOY)
$\eta_1 = 1.9B$	OWSCs (Langlee) Floating

(s) is the Wave period, H (m) is the significant wave height and L_{max} (m) is the Absorption width at maximum power. However, the average power transferred from the water to the converter is generally determined using Eq. (2):

$$P = \iint_{S_B} \left(\frac{1}{T} \int_0^T p \frac{\partial \phi}{\partial n} dt \right) dS \tag{2}$$

where ω (rad/s) is the angular frequency, S_B is the control level of the wetter part of the device, and ϕ is the real velocity potential.

According to the theory of linear potential and analytical solution of integral (2), the average power absorbed by the converter by Eq. (2) is equal to the average power extracted by the wave. The average power extracted from a wave can be written as the product of the average energy flux of the wave (j) within the power absorption (w) Eq. (3):

$$P = WJ \tag{3}$$

where w (m) is capture width of the converter and J (kg m/s^3) is the average energy flux. The average energy flux (J) is written using the wave potential as Eq. (4):

$$J = \frac{1}{2}.C_g.\rho.g.|A_0|^2 \tag{4}$$

where A_0 (m) is the wave amplitude and Cg (m/s) is the group speed parameter written as Eq. (5):

$$C_g = \frac{d\omega}{dk} = \frac{\omega}{2k}\left(1 + \frac{2kh}{\sinh(2kh)}\right) \tag{5}$$

where k (rad/m) is the wave number, and h (m) is the bed depth (Stansell and Pizer, 2013). To calculate the recording width,

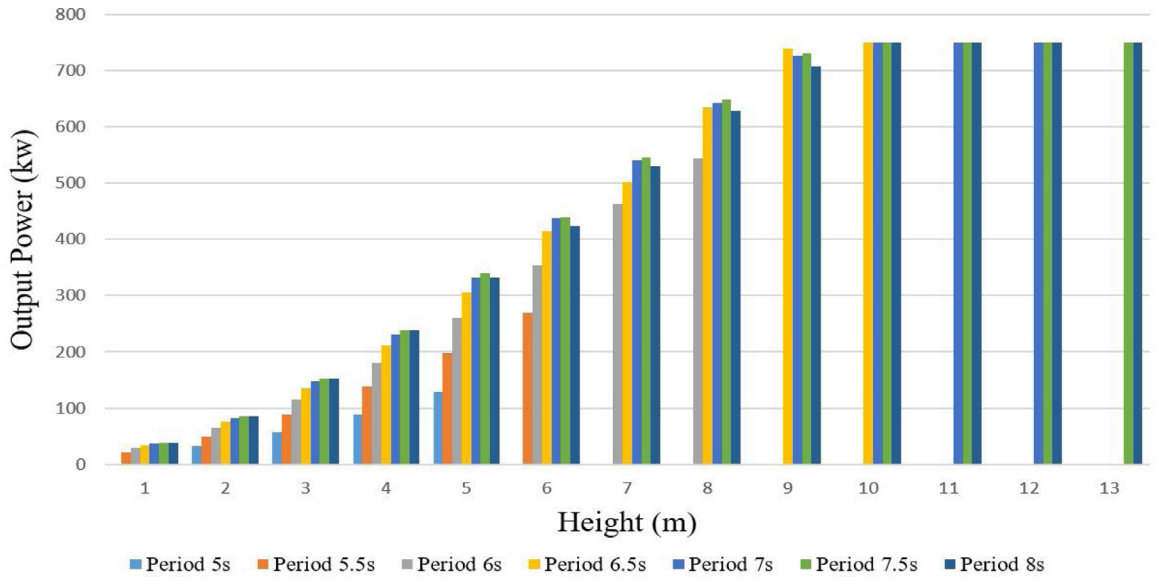

Fig. 5. Pelamis power curve in terms of wave height in different periods (Google Scholar, 0000).

given that the energy absorbed by the transducer is often expressed as the transmitter recording width; this parameter is the width of the input wave that represents the power absorbed by the converter. According to the mathematical Equations governing this aspect of the converter behavior, the final absorption width in a given state is a function of the input wavelength. For this reason, the ultimate absorption potential for a given configuration is usually expressed as a fraction of the wavelength. The formula for calculating the recording width is obtained according to Eq. (6):

$$W = \varepsilon \frac{\lambda}{2\pi} \tag{6}$$

where λ (m) is the wavelength, ε is a coefficient dependent on the propagating field waveform pattern and, thus the degree of freedom. If the system is floating, the field component of the radiation wave has a circular pattern, and the coefficient ε will be equal to 1. W (m) is the absorption width of the device.

Over the recording width is the hydrodynamic efficiency that best reflects the WEC hydrodynamic performance. The measure of hydrodynamic efficiency is CWR, which is obtained by dividing the recording width by a specific dimension B of the WEC and often the device's width. The CWR, denoted by $\eta 1$, absorbs the fraction of wave power flowing through the device that is absorbed by the device Eq. (7):

$$\eta_1 = \frac{W}{B} \tag{7}$$

where B is the characteristic dimension of the device (Babarit, 2015). Finally, the approximate power of the wave converter is calculated from Eq. (8):

$$P = \frac{1}{8}.C_g.\rho.H^2.B.\eta_1 \tag{8}$$

where η_1 is the hydrodynamic efficiency and P is the average power transferred from water to the wave energy converter. Table 2. Shows the appropriate range η_1 for different types of WEC systems (Babarit, 2015):

2.5.1. Pelamis converter

The Pelamis wave energy converter is based on the linear absorber principle; this means that a stretched structure perpendicular absorbs the waves to the wave front. This absorption method allows the highest power absorption without relying on fixed frames and seabed construction. This is the main competitive advantage offered by the Pelamis converter. It is similar to the advantage of all Scenarios wind turbines that use elevators to drive the rotor, unlike previous designs that used traction to drive the rotor. This device can also be used at a depth of 50 to 60 m (Yemm et al., 2012). The output power of the Pelamis converter is shown in Eq. (9) (Babarit, 2015):

$$P = \frac{1}{8}.C_g.\rho.H^2.B.\,(0.21) \tag{9}$$

It is necessary to mention that Eq. (9) is obtained in theory and according to the physical condition of the device studied in the laboratory. In some cases, the Power production may not follow Eq. (9).

The acceptable output power of a Pelamis wave energy converter depends on two main factors, including wave height and wavelength. This study is based on changes in hourly wave height considering a medium period of waves with the significant height that have the greatest impact on electricity generation using the Pelamis device. The conversion of the Pelamis output power matrix to its equivalent power curve, according to the wave conditions, is shown in Fig. 5 (Jahangir et al., 2020b).

2.5.2. WaveStar converter

The WaveStar device consists of floating arms attached to a central retainer and anchored to a seabed. The operation of the generator is done by pressing the hydraulic fluid on the hydraulic motor. In addition, all moving parts are located above the water line. It should be noted that if the weather is stormy, the vessels will move from the water to a safe area. The number of rows of the main part of the device and the number of floating rows can determine the power capacity. In addition, the power of this device is 600 kW.

It should be noted that the recommended installation depth of this converter is more than 50 m (O'Connor et al., 2013). The characteristic surface area is about 4350 m^2, and the characteristic mass is about 1600 tons (Babarit et al., 2012). The output power (Babarit, 2015) and the power curve of this converter are shown in Eq. (10) and Fig. 6.

$$P = \frac{1}{8}.C_g.\rho.H^2.B.\,(0.15) \tag{10}$$

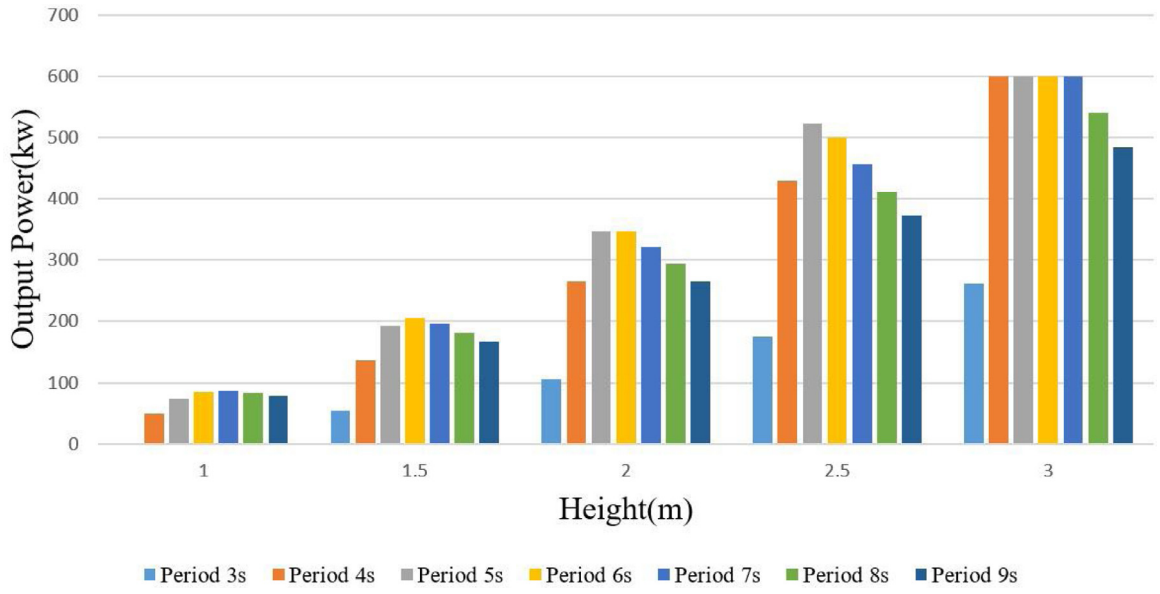

Fig. 6. Wavestar power curve in terms of wave height in different periods (Wavestar, 0000).

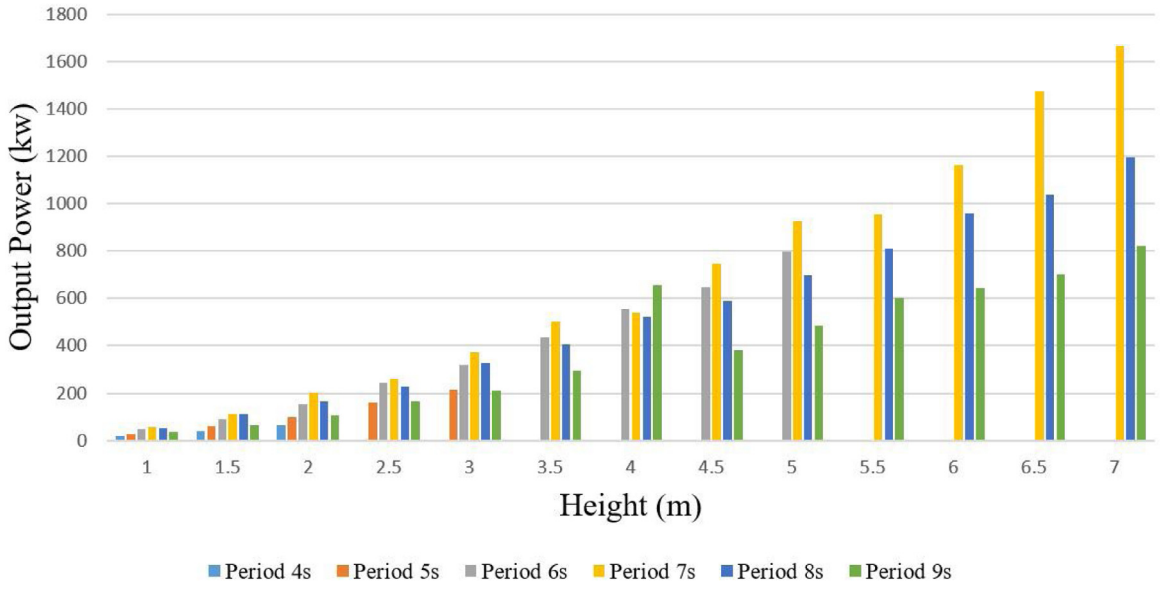

Fig. 7. Langlee power curve in terms of wave height in different periods (Bozzi et al., 2018).

2.5.3. Langlee converter

The Langlee wave energy converter is a floating device that uses the horizontal movements of the wings of vertical water waves. The water wing system is also used by other companies such as E.W. Energy, OVA, and Aquamarine Power is also used. The Langlee wave energy converter consists of four hinged flaps, all connected to a frame. Through PTO systems, the relative motion between each flap and the main frame is converted into useful energy. The characteristic mass of the flaps and the support structure is then estimated at 1600 tons. The characteristic area is about 2200 m^2. In addition, the floating structure allows it to be used in more remote coastal areas (Babarit et al., 2012). This technology has been patented in ten countries around the world. This converter is used in waters with a depth of more than 50 m (PDF, 0000). The output power (Babarit, 2015) and the power curve of this converter are shown in Eq. (11) and Fig. 7:

$$P = \frac{1}{8}.C_g.\rho.H^2.B.\ (0.12) \tag{11}$$

2.5.4. SPA-OWC converter

A new wave energy converter called a floating point absorber using an oscillating water column (SPA-OWC) has been introduced. The OWC-SPA is a point-absorbing converter, also known as an oscillating column. These devices, connected to the seabed, are mainly submerged and symmetrical. The shear pressure generates the force by pressing water into the cylindrical column, which generates a flow of water to move the turbine. Also, the SPA-OWC air chamber is not exposed to the atmosphere, so there are no restrictions on the installation site. This means that the device can be floating or submerged. In addition, the SPA-OWC is not essentially required for high-altitude movement. Therefore, easy access to maintenance is possible (Apparatus and theory, 0000). The output power (Babarit, 2015) and the power curve of this converter are shown in Eq. (12) and Fig. 8.

$$P = \frac{1}{8}.C_g.\rho.H^2.B.\ (0.58) \tag{12}$$

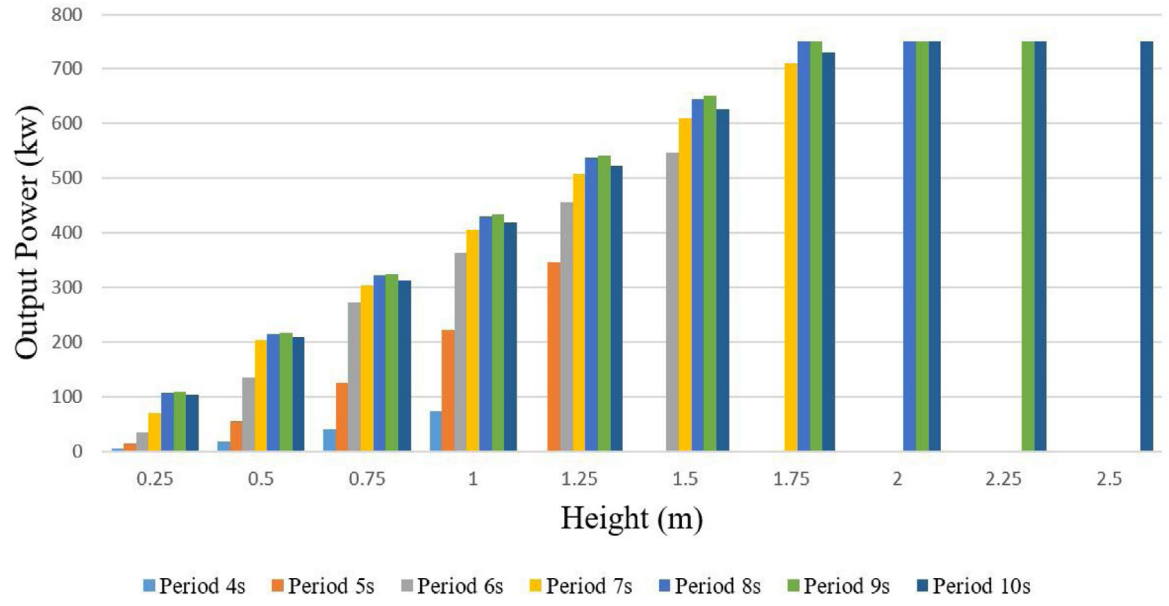

Fig. 8. SPA-OWC power curve in terms of wave height in different periods (Rashid et al., 2011).

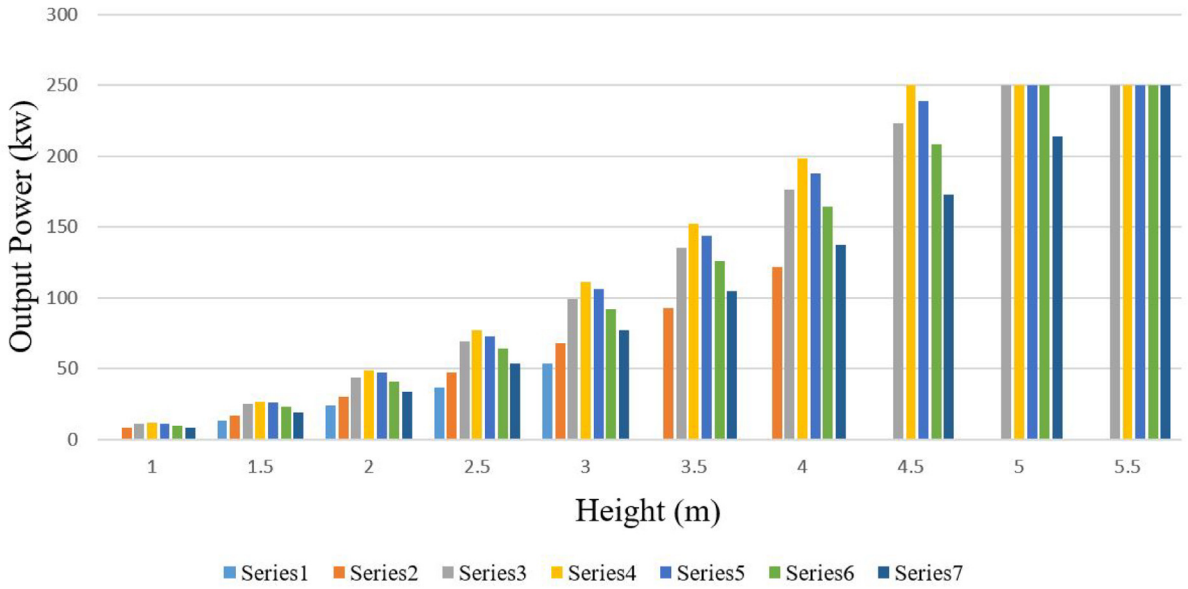

Fig. 9. AquaBuOY power curve in terms of wave height in different periods (Bozzi et al., 2018).

2.5.5. AquaBuOY converter

The next generation AquaBuOY is a technology based on the IPS point absorber system and hose pump made in Sweden. Aqua Energy Group Lt, USA, in collaboration with RAMBOLL Denmark, is developing this system at depths between 15 and 50 m. This system does not need to react against the seabed, so it can be installed in deep water (AquaEnergy Group Lt, 0000). The role of the mooring system is to counteract the thrust and flow forces, so the weight of the anchors and anchors is expected to be low, so it was not considered in the level and mass estimation of the system. Then the characteristic mass is about 5700 tons, and the surface area is about 2100 m^2 (Babarit et al., 2012). The power output (Babarit, 2015) and the power curve of this converter are shown in Eq. (13) and Fig. 9:

$$P = \frac{1}{8} \cdot C_g \cdot \rho \cdot H^2 \cdot B \cdot (0.26) \tag{13}$$

Finally, other information on the five wave energy converters, such as Technical and financial information, is shown in Table 3. This information is beneficial in comparing five-wave converters.

2.6. Selection of components

The other equipment selected for use in the energy system and the most important Equation used by HOMER software for each of these components are introduced. Devices are selected based on availability in target areas. It should be noted that prices are adjusted according to the local market conditions of the study area.

2.6.1. Photovoltaic panel

The solar panel is used to convert solar radiation into electricity. The system's output power depends not only on the intensity

Table 3
Technical and economic information of five wave converters.

Wave converter	Economical			Technical			Ref.
	Capital cost ($)	Replacement cost ($)	O&M cost ($)	Lifetime	Country	Structure	
Langlee	4.812.000	4.120.000	240.560	20	Norway	Floating three-body oscillating flap device	Chang et al. (2018)
Pelamis	4.750.000	4.200.000	443.900	20	Scotland	Bottom-fixed heave-buoy array	Google Scholar (0000)
Wavestar	3.720.000	3.162.000	186.000	20	Denmark	Bottom-fixed heave-buoy array	O'Connor et al. (2013)
AquaBuoy	1.125.000	1.000.000	38.500	20	Finland	Floating two-body heaving converter	Chang et al. (2018)
SPA-OWC	4.815.000	4.477.500	240.750	20	Scotland	Floating oscillating water column	Analysis of Cost Reduction Opportunities (0000)

of the radiation reaching the panel surface but also on the ambient temperature. According to Eq. (14), As the temperature increases, the efficiency of solar panels decreases.

$$P_{PV} = P_{r.PV} \times f_d \times \frac{G}{G_T} \times [1 + \alpha(T_c - 25)] \tag{14}$$

In this Equation, G is solar radiation in terms of w/m^2, Gr is the reference radiation which is equivalent to 21,000 w/m, Pr.PV is the rated power of the photovoltaic module, f_d, the modulus of degradation, α is the temperature coefficient (°C/%), and Tc is the temperature of cells in terms of °C (Vaziri Rad et al., 2020).

2.6.2. Wind turbine

Wind turbine output power is directly related to wind speed. Due to the relatively high load capacity of electricity, a high-capacity wind turbine was selected. Eq. (15) shows the output power of the wind turbine.

$$P_{WT} = \begin{cases} \beta \times P_{Rated} & , V_{Cutin} < V \le V_R \\ P_{Rated} & , V_R < V \le V_{Cutoff} \\ 0 & , V > V_{Cutoff} \text{ or } V < V_{Cutin} \end{cases} \tag{15}$$

In this Eq. is P_{Rated} wind turbine power, V_{Cutin} is the wind speed required to start the turbine, V_{Cutoff} is the speed at which the turbine stops, VR is the wind speed required to produce the rated power by the turbine, V is the wind speed, β Is also calculated by Eq. (16) (Amrollahi and Bathaee, 2017).

$$\beta = \left(\frac{V^3 - V_{Cutin}^3}{V_{Rated}^3 - V_{Cutin}^3} \right) \tag{16}$$

2.6.3. Battery

Lithium-ion batteries can be used for hybrid power systems due to their optimal storage capacity and large-scale development. These systems are used to standardize the electricity generated by other equipment as well as to store energy for peak power consumption times. The output power of the battery is proportional to its discharge power, which can be calculated by Eq. (17):

$$P_{Bat}(t) = E_{Bat}(t-1) \cdot (1-\sigma) - \left(\frac{E_{req}(t)}{\eta_{inv}} - E_{gen}(t) \right) \tag{17}$$

where E_{Bat} is the battery energy at each stage, σ is the rate of automatic discharge, E_{req} is the energy required at a particular time, E_{gen} is the energy produced by the renewable components and diesel generator, and η_{inv} is the efficiency of the inverter (Diaf et al., 2008).

2.6.4. Generator

Implementing diesel generators in off-grid systems helps cover the peak load and reduce the need for batteries, which saves money. Meanwhile, limited fuel consumption and pollution have always been challenging. Energy consumption by diesel generators is calculated by Eq. (18):

$$F_{Dgen}(t) = C_1 \cdot P_R + C_2 \cdot P(t) \tag{18}$$

While FD_{gen} (t) diesel fuel consumption in terms of (l/s), P_t diesel generator power at each stage, PR diesel generator power output, and C1, C2 are fixed parameters, their values are 0.08, and 0.25, respectively (Vaziri Rad et al., 2020).

2.6.5. Converter

Since the solar panel power supply and DC battery storage are considered, inverters are responsible for converting DC to AC and vice versa. The output power of the inverter is calculated using Eq. (19):

$$P_{inv} = \frac{P_{peak}}{\eta_{inv}} \tag{19}$$

Here P_{peak} is the peak load, and η_{inv} is the inverter efficiency (Jahangir et al., 2019).

Other technical and economic specifications of diesel generators, photovoltaic panels, wind turbines, batteries, and converters are shown in Table 4:

2.7. Economic parameters

One of the main challenges in using renewable resources, especially wave converters, is their economic justification. Therefore, the analysis of economic parameters is fundamental. According to the Central Bank of Iran, the inflation rate and discount rates are 15% and 18% (Central Bank of Iran, 0000). Diesel fuel price is considered 0.1$ per liter (Jahangir et al., 2019). The project life of 20 years is equivalent to the life of the main power generation equipment used. This minimizes the impact of changes in equipment replacement costs on the final results.

2.7.1. Economic equations

Cost of energy (COE) and net present cost (NPC) are the two main optimization objectives of this study, which are calculated based on the HOMER optimization algorithm. It should be noted that the accuracy and reliability of the tool have been confirmed by many studies (Sinha and Chandel, 2014). In addition, technical and environmental factors are used to introduce the optimal hybrid energy system. NPC is calculated by combining system capital, replacement, and maintenance costs (including other possible costs such as emission fines or fuel costs) minus the savings (residual value of all components at the end of the project life). Eq. (20) refers to this value over the project's life (Das et al., 2019).

$$NPC = \frac{C_{total}}{CRF\ (i, n)} \tag{20}$$

where C_{total} and CRF are calculated by Eqs. (21), (22):

$$C_{Total} = C_{Capital} + C_{Replacement} + C_{Maintenance} + C_{Salvage} \tag{21}$$

$$CRF\ (i, n) = \frac{i\left(1 + \frac{i-f}{1+f}\right)^n}{\left(1 + \frac{i-f}{1+f}\right)^n - 1} \tag{22}$$

Table 4
Economic data for system components.

	Rated capacity	Capital cost ($)	Replacement cost ($)	O&M cost ($)	Lifetime (year)	Ref.
PV	0.250 kw	1100/kw	1100/kw	10/kw	20	Li et al. (2018) and Tribioli and Cozzolino (2019)
WT	250 kw	362.500	312.500	7.500	20	Baek et al. (2016)
DG	400 kw	1000/kw	900/kw	0.10/kw	20	Muh and Tabet (2019)
Converter	250–1665 kw	550/kw	550/kw	10/year	15	Akhtari and Baneshi (2019)
Battery	100 kwh	20.000	18.000	300	15	Jahangir et al. (2020b)

Table 5
Techno economical specifications of optimal scenarios for limited generators conditions.

System	PV (kW)	WT (Unit)	WEC (Unit)	Bat (Unit)	CON (kW)	DFC (L/year)	COE ($/kWh)	NPC (M$)	IC (M$)	RF (%)
PV/DG/Wavestar	1510		1	62	1306	147 576	0.224	11	6.99	82.1
PV/WT/DG/Wavestar	1418	1	1	57	1235	145 099	0.226	11.1	7.12	82.4
PV/WT/DG/AquaBuOY	1631	1	3	75	1209	159 031	0.227	11.2	7.42	80.7
PV/DG/AquaBuOY	1981		3	86	1285	119 402	0.229	11.3	7.71	85.5
PV/DG/SPA-OWC	1131		1	48	1301	115 687	0.235	11.6	7.17	86
PV/WT/DG/SPA-OWC	1097	1	1	45	1298	101 446	0.240	11.8	7.43	87.7
PV/WT/AquaBuOY	3076	2	3	95	1627	0	0.265	13.1	9.6	100
PV/AquaBuOY	3304		3	116	1762	0	0.268	13.2	9.62	100
PV/Wavestar	3327		1	105	1663	0	0.276	13.6	9.65	100
PV/DG/Langee	1817		1	83	1315	121 157	0.276	13.6	8.63	85.3
PV/WT/Wavestar	3193	1	1	102	1661	0	0.280	13.8	9.80	100
PV/WT/DG/Langee	1802	1	1	81	1295	96 182	0.280	13.8	8.93	88.3
PV/WT/SPA-OWC	2425	1	1	87	1643	0	0.291	14.3	9.53	100
PV/SPA-OWC	2870		1	92	1581	0	0.295	14.5	9.72	100
PV/Langee	3246		1	107	1710	0	0.315	15.5	10.5	100
PV/WT/Langee	3037	1	1	106	1708	0	0.318	15.7	10.6	100
PV/DG/Pelamis	1986		1	91	1314	125 078	0.335	16.5	8.93	84.4

Table 6
Techno economical specifications of optimal scenarios for unlimited generators conditions.

System	PV (kW)	WT (Unit)	WEC (Unit)	Bat (Unit)	CON (kW)	DFC (L/year)	COE ($/kWh)	NPC (M$)	IC (M$)	RF (%)
PV/DG/AquaBuOY	1538		3	65	779	235 452	0.209	10.3	6.97	71.4
PV/WT/DG/AquaBuOY	1376	1	3	59	765	242 208	0.210	10.4	6.98	70.6
PV/DG/Wavestar	974		1	38	753	291 075	0.212	10.4	6.02	64.7
PV/WT/DG/Wavestar	1144	1	1	48	782	199 391	0.216	10.6	6.79	75.8
PV/DG/SPA-OWC	844		1	25	755	205 642	0.221	10.9	6.50	75.1
PV/WT/DG/SPA-OWC	698	1	1	29	653	186 368	0.223	11	6.72	77.4
DG/SPA-OWC			1	44	734	441 272	0.236	11.6	5.94	46.5
WT/DG/Wavestar		3	1	46	748	475 689	0.244	12	6.20	42.3
WT/AquaBuOY	3076	4	3	49	731	603 856	0.249	12.2	6.33	26.7
PV/DG/Langee	1327		1	60	765	267 981	0.261	12.9	7.73	67.5
PV/WT/DG/Langee	1254	1	1	59	745	239 746	0.264	13	7.98	70.9
DG/WT/Langee		3	1	51	734	621 858	0.298	14.7	7.16	24.5
PV/DG/Pelamis	1631		1	67	783	247 584	0.332	15.9	8.16	70
PV/DG/WT/Pelamis	1550	1	1	66	763	212 047	0.324	16	8.44	74.3
DG/WT/Pelamis		4	1	48	743	638 111	0.362	17.8	7.42	22.6

where Ct is the total cost in terms of $/year, CRF is the return on investment i'' nominal interest rate, f is the inflation rate and n is the number of years (Rad et al., 2020). Also, the value of scrap value can be calculated by Eq. (23):

$$C_{Salvage} = C_{\text{Replacement}} \times \frac{R_{Component} - \left(R_{\text{Pr}\,oject} - R_{Component}.INT\left(\frac{R_{\text{Pr}\,oject}}{R_{Component}}\right)\right)}{R_{Component}} \tag{23}$$

R in the above Eq. represents longevity.

Finally, COE is the cost of useful energy per kilowatt hour and one of the most important parameters in finding cost-effective hybrid energy systems (Eserved); Which is calculated by Eq. (24) (Das et al., 2019).

$$COE = \frac{C_{Total}}{E_{Ser\,ved}} \tag{24}$$

3. Results and discussion

Tables 5 and 6 describe the proposed system based on wave converters in two generator scenarios. The effect of superior wave converters on electricity generation compared to other components is also presented. Finally, sensitivity analysis on initial costs, replacement and maintenance is performed.

In these proposed systems, the generator is placed as a member of the system responsible for the production of 20% of the island's demand to increase the system's stability and reliability. Also, the generator enters the circuit at its maximum capacity. In this case, according to the wave potential of Lavan Island, the amount of solar radiation and wind radiation is considered the most suitable combined system of power, photovoltaic panel, diesel generator, and Wavestar wave converter with a cost of energy of 0.224 $/kWh. Thus, in the optimal scenario, out of the five converters selected, the Wavestar wave converter has the lowest cost of energy (COE) and net current cost (NPC). However,

Table 7
Hourly power consumption diagram by system components for different.

limited generator scenario	unlimited generator scenario
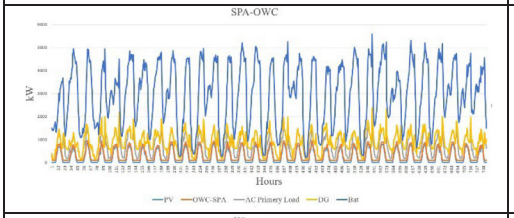	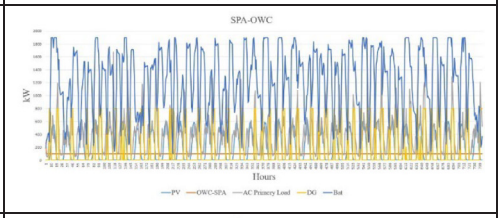
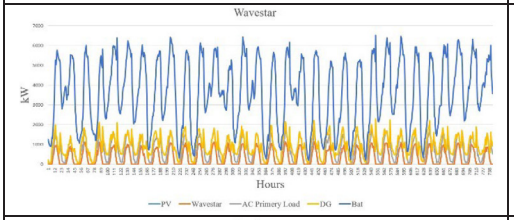	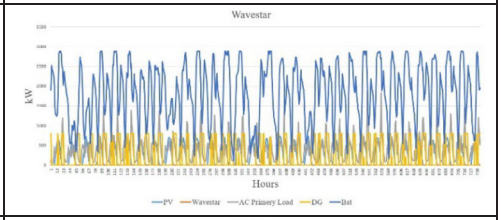
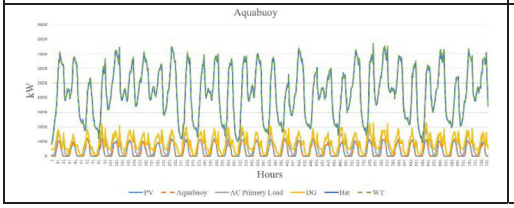	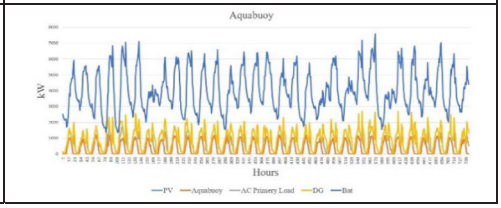

this calculation is done in a situation where there is a limit for the generator, and the percentage of renewable energy use in any of the scenarios is not less than 82.1%. This decision may increase the cost of our system a little, but it will also reduce emissions from burning diesel in the generator. As shown in Table 5, photovoltaic panels and the WEC system are present in all scenarios. Also, among the five selected wave converters, Wavestar, AquaBuOY, SPA-OWC, Langlee, and Pelamis converters have the largest share in the optimal scenarios, respectively.

Table 6. does not have a limit for the generator, and the generator can supply up to half of the electricity demand. As can be seen, NPC and COE costs are generally reduced slightly, but pollution will increase due to the use of diesel fuel for the generator. In this case, the AquaBuOY converter in combination with a photovoltaic panel and diesel generator with cost of energy of 0.209 $/kWh and net present cost of 10.3 M$ has been selected as the most optimal scenario. It is seen that giving more shares to the generator will reduce the NPC by 700,000 $, but the initial cost will not be much different. The combination of AquaBuOY converter, photovoltaic panel, diesel generator, and wind turbine with COE 0.210 $/kWh and NPC 10.4 million $ and the combination of Wavestar converter, generator, and photovoltaic panel with COE and NPC $ 0.212 and 10.4 million dollar respectively will be our three optimal scenarios. Also, as in the previous scenario, the Pelamis converter was ranked last in the most optimal scenario among the five wave converters selected in this project. The combination of Pelamis converter with wind turbine and diesel generator with NPC 17.8 M$ and COE 0.362 $/kWh is the most expensive combination among other favorable scenarios. Other technical and economic specifications are shown in Table 6.

Thus, among the above converters, the results of the three converters, Wavestar, AquaBuOY, and SPA-OWC, were somewhat similar and were present in the top scenarios. But in addition to the cost, the converter's role in generating the required electricity and other sources is vital. Table 7 shows the contribution of each equipment to electricity production required in the month of peak consumption (July) in both limited and unlimited generator scenarios. In a limited diesel generator scenario, the spa_owc wave energy converter is more efficient than the other two converters, and this converter's power output does not reach zero during July. But the other two converters have almost the same conditions, and their production capacity reaches zero in some hours in July. In an unlimited diesel generator scenario, the spa_owc converter is more stable, despite the amount of power generated by the aqua converter. It should be noted that as can be seen, the View Star converter shows poor performance this month.

One of the most important factors in comparing the efficiency of energy systems is power generation profiles and annual energy production costs. Due to the fact that in the limited Scenario, the Wavestar converter generator was considered the most optimal scenario, and in the unlimited Scenario, the AquaBuOY converter was selected in the optimal scenario, in Table 7. Wavestar and AquaBuOY are displayed in combination with other optimal equipment (see Fig. 10).

As can be seen, the cost of energy of the diesel generator and the photovoltaic panel in both scenarios is the same and equals to 0.024 $/kWh and 0.0394 $/kWh. But wave converters have different cost of energy; So that in the case of constraint for the generator, which Wavestar converter was the most optimal converter in terms of NPC and COE, has cost of energy of 0.385 $/kWh. If the AquaBuOY converter, which is the optimal converter in scenario of unlimited generator, is selected, it has a relatively high cost of energy of 2.05 $/kWh. Other factors that affect the uncertainty of the proposed scenarios include fluctuations in initial costs, replacement, and maintenance. The Net Current Cost (NPC) of the two optimal scenario converters in both generator Scenarios relative to changes in initial cost, device replacement cost, and maintenance cost is shown in Fig. 11. It is observed that if the costs are 1.5 times the initial amount, the net present cost will increase to 13.9 M$. In other words, depending on the range of price changes during the project, the net cost changes can vary from 10.3 M$ to 13.9 M$.

4. Conclusion

Combining energy sources leads to a higher, cleaner, and more efficient power supply. This study, a Feasibility study of operating

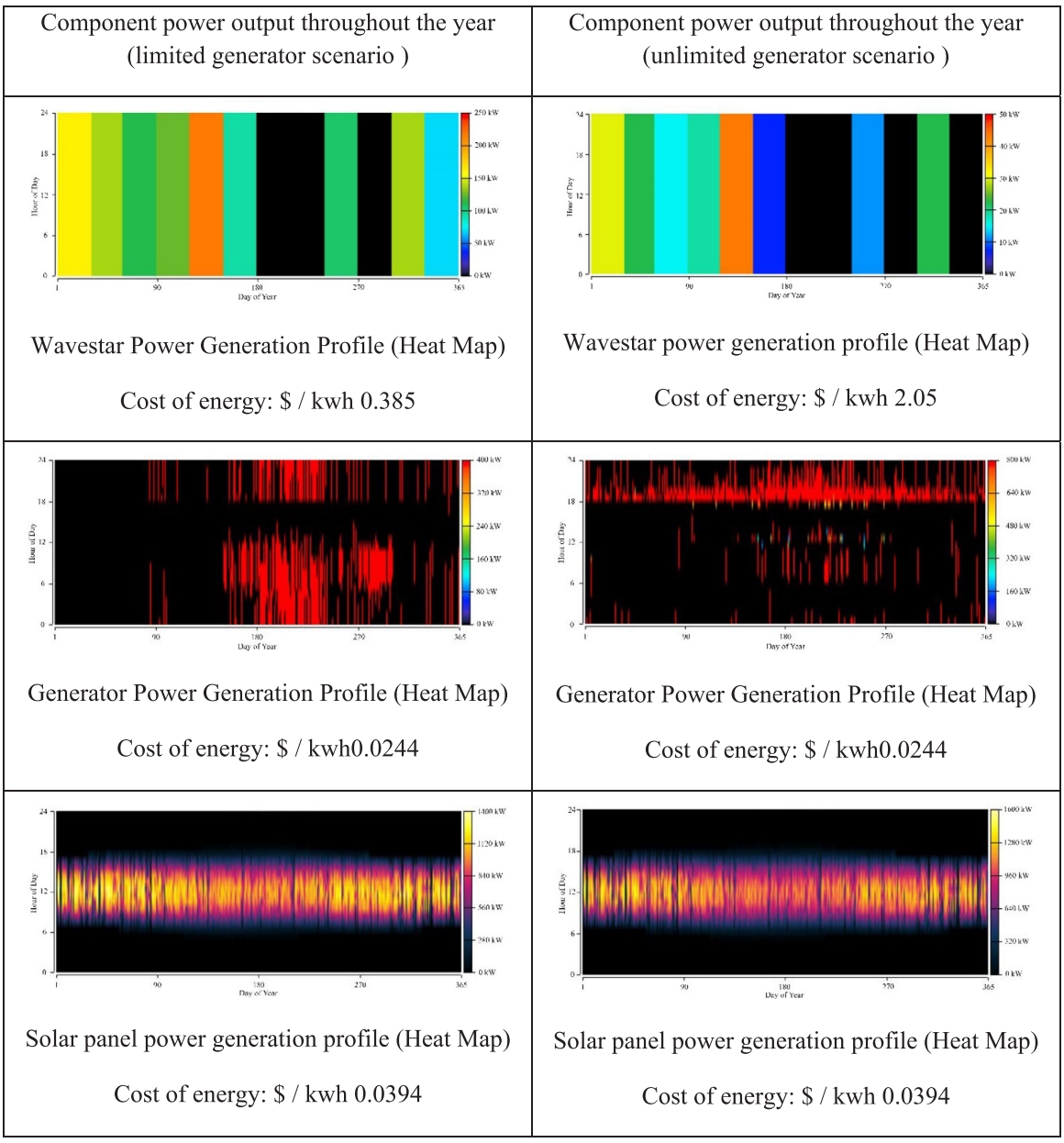

Fig. 10. Production power Specifications of Wavestar, diesel generator and photovoltaic panel for the generator with restrictions.

five types of wave energy converters to achieve the optimal hybrid system including photovoltaic panel, wind turbine, battery, and diesel generator in two limited and unlimited Scenarios for the generator to improve the performance of the hybrid system was investigated. Finally, sensitivity analysis was performed on the economical parameters of optimal wave converters. The most important results are as follows:

- In the case of limiting the use of diesel generator fuel, the combined system, including photovoltaic panel, diesel generator, and wavestar wave energy converter, with an energy cost of 0.224 $ per kWh and a net present cost of 11 million $, was selected as the most optimal combination. It should be noted that in this case, the percentage of use of renewable resources will be equal to 82.1%.
- On the other hand, when the diesel generator is allowed to provide up to half of the required power, the combined system, including the photovoltaic panel, diesel generator, and AquaBuOY wave energy converter, has an energy cost of 0.209 $/kWh and a net present cost of 10.3 million $. Dollars were chosen as the most suitable system. In this scenario, the percentage of use of renewable equipment was reported as 71.4% due to the removal of the previous state restriction for using diesel generators.
- In the combined system, including the Wavestar wave energy converter, the energy production cost by this converter was 0.385 $/kWh. While in the integrated system, including the AquaBuOY converter, this amount was measured as 2.05 $/kWh.
- Another critical goal of this study was to investigate the contribution of power generation by wave energy converters in different scenarios. In this regard, the SPA-OWC converter had the largest contribution to power generation in the conditions of restriction on the generator and its absence.
- And finally, changes in the costs of the Wavestar and AquaBuOY converters have resulted in changes in the net present cost from 10.3 million dollars to 13.9 million dollars.

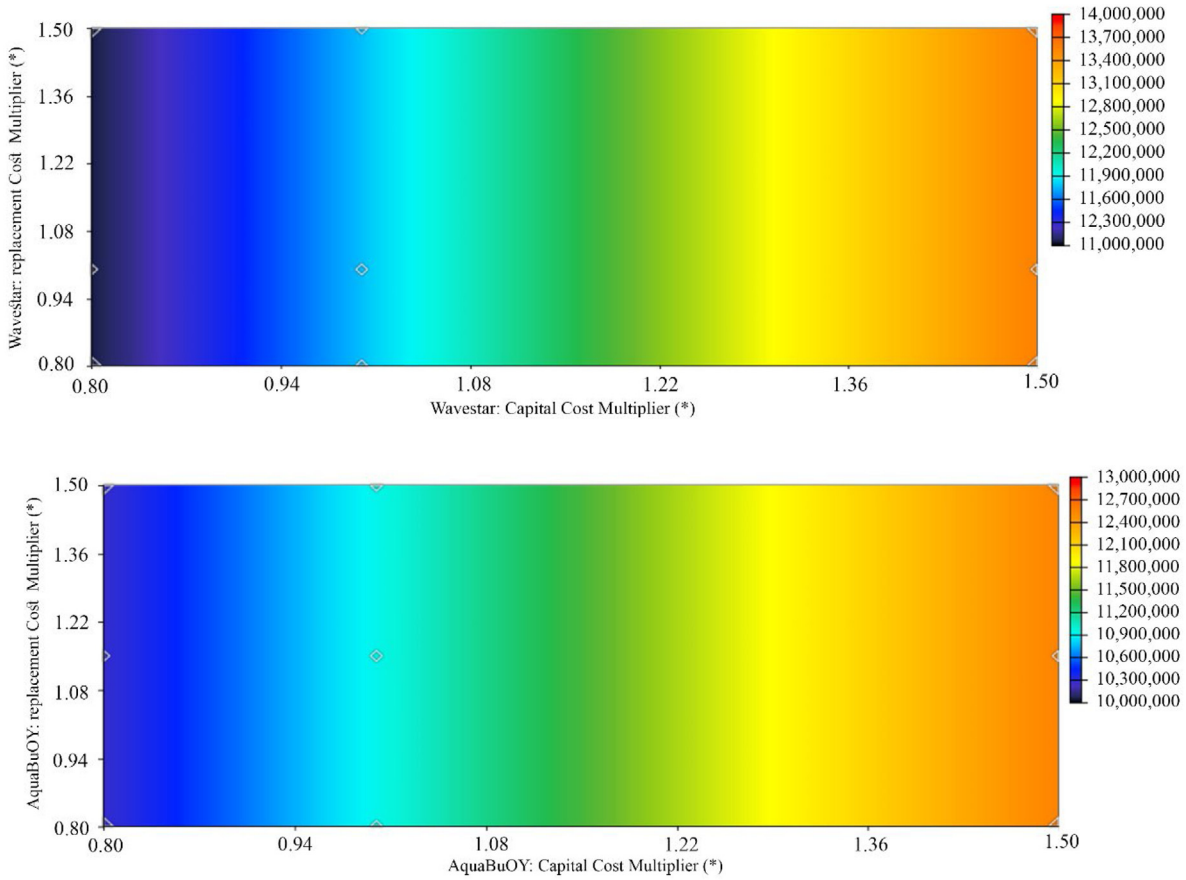

Fig. 11. _ Impact of changes in initial cost and replacement on net present cost.

Declaration of competing interest

The authors declare that they have no known competing financial interests or personal relationships that could have appeared to influence the work reported in this paper.

Data availability

No data was used for the research described in the article.

References

Akhtari, M.R., Baneshi, M., 2019. Techno-economic assessment and optimization of a hybrid renewable co-supply of electricity, heat and hydrogen system to enhance performance by recovering excess electricity for a large energy consumer. Energy Convers. Manag. 188, 131–141. http://dx.doi.org/10.1016/j.enconman.2019.03.067.

Amrollahi, M.H., Bathaee, S.M.T., 2017. Techno-economic optimization of hybrid photovoltaic/wind generation together with energy storage system in a stand-alone micro-grid subjected to demand response. Appl. Energy 202, 66–77. http://dx.doi.org/10.1016/j.apenergy.2017.05.116.

Analysis of cost reduction opportunities in the wave energy industry. - google search.

Andini, C., Cabral, R., Santos, J.E., 2019. The macroeconomic impact of renewable electricity power generation projects. Renew. Energy 131, 1047–1059. http://dx.doi.org/10.1016/j.renene.2018.07.097.

Apparatus and theory of a submerged point absorber using oscillating water column - IEEE conference publication.

Aquaenergy group Lt - google search.

Babarit, A., 2015. A database of capture width ratio of wave energy converters. Renew. Energy 80, 610–628. http://dx.doi.org/10.1016/j.renene.2015.02.049.

Babarit, A., Hals, J., Muliawan, M.J., Kurniawan, A., Moan, T., Krokstad, J., 2012. Numerical benchmarking study of a selection of wave energy converters. Renew. Energy 41, 44–63. http://dx.doi.org/10.1016/j.renene.2011.10.002.

Baek, S., Park, E., Kim, M.G., Kwon, S.J., Kim, K.J., Ohm, J.Y., del Pobil, A.P., 2016. Optimal renewable power generation systems for busan metropolitan city in South Korea. Renew. Energy 88, 517–525. http://dx.doi.org/10.1016/j.renene.2015.11.058.

2011. From blue to green. IEEE Control Syst. 31, 18–24. http://dx.doi.org/10.1109/MCS.2011.941960.

Bozzi, S., Besio, G., Passoni, G., 2018. Wave power technologies for the mediterranean offshore: Scaling and performance analysis. Coast. Eng. 136, 130–146. http://dx.doi.org/10.1016/j.coastaleng.2018.03.001.

Carvalho, D.B., Guardia, E.C., Marangon Lima, J.W., 2019. Technical-economic analysis of the insertion of PV power into a wind-solar hybrid system. Sol. Energy 191, 530–539. http://dx.doi.org/10.1016/j.solener.2019.06.070.

Central bank of iran - google search.

Chang, G., Jones, C.A., Roberts, J.D., Neary, V.S., 2018. A comprehensive evaluation of factors affecting the levelized cost of wave energy conversion projects. Renew. Energy 127, 344–354. http://dx.doi.org/10.1016/j.renene.2018.04.071.

Das, B.K., Al-Abdeli, Y.M., Woolridge, M., 2019. Effects of battery technology and load scalability on stand-alone PV/ICE hybrid micro-grid system performance. Energy 168, 57–69. http://dx.doi.org/10.1016/J.ENERGY.2018.11.033.

Diaf, S., Notton, G., Belhamel, M., Haddadi, M., Louche, A., 2008. Design and techno-economical optimization for hybrid PV/wind system under various meteorological conditions. Appl. Energy 85, 968–987. http://dx.doi.org/10.1016/j.apenergy.2008.02.012.

Energy National Balance Sheet of Iran for 2016, 2016. Minist. Energy-2019 - google search.

Fakouriyan, S., Saboohi, Y., Fathi, A., 2019. Experimental analysis of a cooling system effect on photovoltaic panels' efficiency and its preheating water production. Renew. Energy 134, 1362–1368. http://dx.doi.org/10.1016/j.renene.2018.09.054.

google map - Google Search, https://www.google.com/search?q=google+map&oq=google+map&aqs=chrome..69i57j0i512l4j69i65j69i60l2.9740j0j7&sourceid=chrome&ie=UTF-8.

Cost analysis of wave energy in the Pacific - google scholar.

https://www.amar.org.ir - google search.

Haryuda, S.I., Susila, I.W., Siregar, I.H., Aris, A., 2019. Power control of grid-connected photovoltaic-wind turbin-bouy conversion energy wave hybrid system. In: IOP Conference Series: Materials Science and Engineering. Institute of Physics Publishing, 012074.

HOMER pro user manual.
The overview of INCOD.
Jahangir, M.H., Fakouriyan, S., Vaziri Rad, M.A., Dehghan, H., 2020a. Feasibility study of on/off grid large-scale PV/WT/WEC hybrid energy system in coastal cities: A case-based research. Renew. Energy 162, 2075–2095. http://dx.doi.org/10.1016/j.renene.2020.09.131.
Jahangir, M.H., Khatibi, A., 2020. Site selection of harmonic pressure water energy convertor systems on the south coast of the Caspian sea using cluster analysis. Sustain. Energy Technol. Assess. 38, 100678. http://dx.doi.org/10.1016/j.seta.2020.100678.
Jahangir, M.H., Mazinani, M., 2020. Evaluation of the convertible offshore wave energy capacity of the southern strip of the Caspian sea. Renew. Energy 152, 331–346. http://dx.doi.org/10.1016/j.renene.2020.01.012.
Jahangir, M.H., Mousavi, S.A., Vaziri Rad, M.A., 2019. A techno-economic comparison of a photovoltaic/thermal organic rankine cycle with several renewable hybrid systems for a residential area in Rayen. Iran. Energy Convers. Manag. 195, 244–261. http://dx.doi.org/10.1016/j.enconman.2019.05.010.
Jahangir, M.H., Shahsavari, A., Vaziri Rad, M.A., 2020b. Feasibility study of a zero emission PV/Wind turbine/wave energy converter hybrid system for stand-alone power supply: A case study. J. Clean. Prod. 262, 121250. http://dx.doi.org/10.1016/j.jclepro.2020.121250.
Kamranzad, B., Chegini, V., 2014. Study of wave energy resources in Persian gulf : Seasonal and monthly distributions. In: 11th Int. Conf. Coasts, Ports Mar. Struct. (ICOPMAS 2014). pp. 658–661. http://dx.doi.org/10.13140/RG.2.1.2990.2249.
Krozer, Y., 2013. Cost and benefit of renewable energy in the European union. Renew. Energy 50, 68–73. http://dx.doi.org/10.1016/j.renene.2012.06.014.
Lavan Island - wikipedia.
Laws, N.D., Epps, B.P., 2016. Hydrokinetic energy conversion: Technology, research, and outlook.
Li, Y., Gao, W., Ruan, Y., 2018. Performance investigation of grid-connected residential PV-battery system focusing on enhancing self-consumption and peak shaving in Kyushu. Japan. Renew. Energy 127, 514–523. http://dx.doi.org/10.1016/j.renene.2018.04.074.
Lund, H., 2006. Large-scale integration of optimal combinations of PV, wind and wave power into the electricity supply. Renew. Energy 31, 503–515. http://dx.doi.org/10.1016/j.renene.2005.04.008.
Middleton, P., 2018. Sustainable living education: Techniques to help advance the renewable energy transformation. Sol. Energy 174, 1016–1018. http://dx.doi.org/10.1016/j.solener.2018.08.009.
Muh, E., Tabet, F., 2019. Comparative analysis of hybrid renewable energy systems for off-grid applications in southern Cameroons. Renew. Energy 135, 41–54. http://dx.doi.org/10.1016/j.renene.2018.11.105.
Nasa, 2019. NASA surface meteorology and solar energy - google scholar.
Ocean wave energy: current status and future prespectives - Joao Cruz - google books.
O'Connor, M., Lewis, T., Dalton, G., 2013. Techno-economic performance of the pelamis P1 and wavestar at different ratings and various locations in Europe. Renew. Energy 50, 889–900. http://dx.doi.org/10.1016/j.renene.2012.08.009.
(PDF) results of an experimental study of the langlee wave energy converter.
Rad, M.A.V., Ghasempour, R., Rahdan, P., Mousavi, S., Arastounia, M., 2020. Techno-economic analysis of a hybrid power system based on the cost-effective hydrogen production method for rural electrification, a case study in Iran. Energy 190, 116421. http://dx.doi.org/10.1016/J.ENERGY.2019.116421.
Rashid, A., Reviews, S.H.-R., E, S., 2011. Undefined: Status and Potentials of Offshore Wave Energy Resources in Chahbahar Area (NW Omman Sea). Elsevier.
Reikard, G., Robertson, B., Bidlot, J.R., 2015. Combining wave energy with wind and solar: Short-term forecasting. Renew. Energy 81, 442–456. http://dx.doi.org/10.1016/j.renene.2015.03.032.
Ren21, 2010. Renewables 2010 global status report, 2010 - google scholar.
Ren21, 2019. Renewables 2019 global status report, 2019 - google scholar.
Renewable energy sources and climate change mitigation: special report of... - google books.
Rodriguez-Delgado …, C., of C., R.B.-J., 2019. Undefined: Dual Wave Farms for Energy Production and Coastal Protection under Sea Level Rise. Elsevier.
Sang, Y., Karayaka, H.B., Yan, Y., Zhang, J.Z., Bogucki, D., Yu, Y.H., 2017. A rule-based phase control methodology for a slider-crank wave energy converter power take-off system. Int. J. Mar. Energy 19, 124–144. http://dx.doi.org/10.1016/j.ijome.2017.07.001.
Sinha, S., Chandel, S.S., 2014. Review of software tools for hybrid renewable energy systems.
Stansell, P., Pizer, D.J., 2013. Maximum wave-power absorption by attenuating line absorbers under volume constraints. Appl. Ocean Res. 40, 83–93. http://dx.doi.org/10.1016/j.apor.2012.11.005.
Talaat, M., Farahat, M.A., Elkholy, M.H., 2019. Renewable power integration: Experimental and simulation study to investigate the ability of integrating wave, solar and wind energies. Energy 170, 668–682. http://dx.doi.org/10.1016/j.energy.2018.12.171.
Tribioli, L., Cozzolino, R., 2019. Techno-economic analysis of a stand-alone microgrid for a commercial building in eight different climate zones. Energy Convers. Manag. 179, 58–71. http://dx.doi.org/10.1016/j.enconman.2018.10.061.
Vaziri Rad, M.A., Toopshekan, A., Rahdan, P., Kasaeian, A., Mahian, O., 2020. A comprehensive study of techno-economic and environmental features of different solar tracking systems for residential photovoltaic installations. Renew. Sustain. Energy Rev. 129, 109923. http://dx.doi.org/10.1016/j.rser.2020.109923.
Wavestar.
Wilberforce, T., El Hassan, Z., Durrant, A., Thompson, J., Soudan, B., Olabi, A.G., 2019. Overview of ocean power technology. Energy 175, 165–181. http://dx.doi.org/10.1016/j.energy.2019.03.068.
Yemm, R., Pizer, D., Retzler, C., Henderson, R., 2012. Pelamis: Experience from concept to connection. In: Philosophical Transactions of the Royal Society A: Mathematical, Physical and Engineering Sciences. Royal Society, pp. 365–380.
Zhang, Z.Y., Liu, H.X., Zhang, L., Zhang, W.C., Ma, Q.W., 2018. Study on the performance analysis and optimization of funnel concept in wave-energy conversion. J. Mar. Sci. Technol. 23, 696–705. http://dx.doi.org/10.1007/s00773-017-0504-4.